Journal of Applied Fluid Mechanics, Vol. 11, No. 3, pp. 721-731, 2018.
Available online at www.jafmonline.net, ISSN 1735-3572, EISSN 1735-3645.
DOI: 10.29252/jafm.11.03.28505

Experimental Investigation and Numerical Simulation of Morphological Changes in Natural Channel Bend

S. K. Lee[1†] and T. A. Dang[2]

[1*]*Sustainable Management of Natural Resources and Environment Research Group, Faculty of Environment and Labour Safety, Ton Duc Thang University, Ho Chi Minh City, Vietnam 19, Nguyen Huu Tho Str., Tan Phong Ward, Dist. 7, Ho Chi Minh City, Vietnam*
[2]*University of Science, Vietnam National University, Ho Chi Minh City 227 Nguyen Van Cu Str., 5 Dist., Ho Chi Minh City, Vietnam*

†*Corresponding Author Email: leeseungkyu@tdt.edu.vn*

(Received October 8, 2017; accepted December 23, 2017)

ABSTRACT

Sediment transport is an important process in maintaining balance of the form of river. The transport of bed load particles affects the processes of aggradation and degradation of the riverbed significantly. To predict the evolution process of the river morphology, the numerical model is considered as a useful tool. This study developed a two-dimensional (2D) depth-averaged model for the morphological change in the river bend. The flow module is represented by the shallow water equations, and the river morphological changes are represented by the sediment continuity equation. The sediment transport module treats bed load as mixtures of multiple grain-size sediments. A finite difference method was applied to solving the governing equations. The developed model was applied to predict bed-load transport rate on one set of the laboratory experiment. A field study was further applied to demonstrate the capability of the developed model in predicting morphological change in the curved river section in South Korea. The simulation results of the developed model were in good agreement with field data both laboratory experiment and natural channel bend.

Keywords: Experimental; Numerical model; Bedload; Grain-size; Curved channel.

NOMENCLATURE

A	parameter
d_m	grain size
Dt	time interval
D_x	grid space in the x direction
D_y	grid space in the y direction
f_s	sediment shape factor
g	the acceleration of gravity;
h	water depth
n	Manning's coefficient
p	porosity
q_{tbs}	total bed load discharge
q_x	flow discharge in the x direction
q_y	flow discharge in the y direction
q^*_{sb}	bed load discharge capacity
u	flow discharge in the x direction
v	flow discharge in the y direction
r_s	parameter
S_{fx}	friction bed slope in the x direction
S_{fy}	friction bed slope in the y direction
S_{ox}	bed slope in the x direction
S_{oy}	bed slopes in the y direction
t	time
X_{obs}	measured value
X_{obs}	predicted value
Z_{bi}	riverbed elevation
α	coefficient
β	coefficient
σ_s	the specific gravity
τ_b	bed shear stress
τ_{ci}^*	dimensionless Shields stress

1 INTRODUCTION

Natural channels never stop changing their geomorphic characteristics, especially the flow in meandering channels (Begnudelli *et al.* 2010; Bhallamudi and Chaudhry, 1991). It is considered as the main cause of the aggradation, and degradation of the riverbed (Begnudelli *et al.* 2010; Darby *et al.* 2002). Physical models can be considered as effective tools for testing sediment transport formulae and investigating the processes of river morphology evolution in watersheds

(Darby *et al*. 2002). In recent decades, numerical models have been developed to simulate the bed load discharge based on the combination of laboratory survey and numerical models (Guan *et al*. 2016; Miglio *et al*. 2009). Several studies stated that calculating the sediment transport rate in channels, especially estimating the bed load transport rate in meandering channels, which results in geomorphic changes, is extremely difficult and very expensive. Three-dimensional (3D) models are considered as an optimal choice to simulate bed level variation in natural channel bends, because it can provide more information than depth-averaged 2D model (Kasvi *et al*. 2015; Khosronejad *et al*. 2007; Lane *et al*. 1999; Wang *et al*. 2014). Currently, there are many arguments about the applicability of 2D model for predicting the water level, flow discharge and morphological change in the river bend (Barbhuiya and Talukdar, 2010; Waters and Curran, 2015). Duan (2004) also reported that the effect of secondary flow in some practical cases is not significant when the curvature effect is small. They also reported that a 2D model with the dispersion terms is capable of predicting flow distribution in meandering channels. Waters and Curran (2015) commented that sediment composition greatly affected channel morphology.

However, they also reported that estimating grain sizes spatially in reality is a difficult problem because of the complexity of the riverbed topography. According to Alho and Mäkinen, 2010; Lane *et al*. 1999, 2D model hydrodynamics could simulate the bed level variation reasonably well in a curved river even without the inclusion of a secondary flow correction.

The main objective of this work is to investigate the applicability of the 2D numerical model, which is developed based on the Cartesian coordinate to simulate flow hydrodynamic and bed level variation in curved and straight channels by treating bed load as mixtures of grain-size fraction (Paulo *et al*. 2007; Darby *et al*. 2002; Duan, 2004). The numerical model is written based on the structure of the Fortran program.

The model was first verified through the laboratory experiment of bed degradation in meandering open channel at the hydraulic laboratory of the Research Center for River Flow Impingement and Debris Flow (RCRFIDF), Gangneung-Wonju National University, South Korea. Then, the constructed model is used to

simulate the degradation or aggradation processes of the river bed in the curved river section. Finally, bed level variation predictor of both laboratory experiment case and Eosungjun curved river section were calibrated and verified using field data. The simulation results in both cases are in good agreement with measurement data.

2. METHODOLOGICAL

2.1 Shallow Water Equations

The 2D shallow water equations are expressed in Cartesian coordinates assuming that distribution of pressure is hydrostatic. In addition, turbulence and dispersion terms may have effects on the transport of sediment concentration (Li *et al*. 2011; Guan *et al*. 2016). However, the developed model is constructed based on bed load dominant and only the bed load transport is applied. Therefore, turbulence and dispersion terms were not considered in this study. The governing equations are written in a conservative form as:

$$\frac{\partial h}{\partial t}+\frac{\partial}{\partial x}(q_x)+\frac{\partial}{\partial y}(q_y)=0 \tag{1}$$

$$\frac{\partial}{\partial t}(q_x)+\frac{\partial}{\partial x}\left(\frac{q_x^2}{h}\right)+\frac{\partial}{\partial y}\left(\frac{q_x q_y}{h}\right) = -gh\frac{\partial Z}{\partial x}+\frac{1}{\rho h}\left(\frac{\partial T_{xx}}{\partial x}+\frac{\partial T_{xy}}{\partial y}\right)-\frac{\tau_{bx}}{\rho}+gh\left(S_{ox}-S_{fx}\right) \tag{2}$$

$$\frac{\partial}{\partial t}(q_y)+\frac{\partial}{\partial x}\left(\frac{q_x q_y}{h}\right)+\frac{\partial}{\partial y}\left(\frac{q_y^2}{h}\right) = -gh\frac{\partial Z}{\partial y}+\frac{1}{\rho h}\left(\frac{\partial T_{yx}}{\partial x}+\frac{\partial T_{yy}}{\partial y}\right)-\frac{\tau_{by}}{\rho}+gh\left(S_{oy}-S_{fy}\right) \tag{3}$$

where t is the time; h is the water depth; q_x and q_y are the flow discharge components in the x and y directions, respectively; g is the acceleration of gravity; T_{xx}, T_{xy}, T_{yx}, T_{yy} and S_{ox}, S_{oy} are the depth averaged turbulent stresses and bed slopes of the bed river in the x and y directions, respectively; S_{fx} and S_{fy} are the friction bed slopes, respectively.

$$S_{fx}=\frac{n^2 q_x\sqrt{q_x^{\,2}+q_y^{\,2}}}{h^{\frac{4}{3}}} \tag{4}$$

$$S_{fy}=\frac{n^2 q_y\sqrt{q_x^{\,2}+q_y^{\,2}}}{h^{\frac{4}{3}}} \tag{5}$$

where n is Manning's roughness coefficient.

2.2 Sediment Transport Equations

In most natural rivers, flow regimes are often un-steady (Waters and Curran, 2015).

Bed load in natural rivers especially in steep slope rivers is often distributed with non-uniform size (Guan *et al*. 2016; Dang and Park, 2016b). Therefore applying a bed load transport formula with uniform particle size, the calculated results often differ by orders of magnitude. Guan *et al*. (2016) constructed a 2D numerical model for predict bed deformation and the model is applied to predict bed level variation at natural bends. They reported that grain-size parameters have an important role on bed level variation. Dang and Park (2016b) reported that bed load in the mountain river often distributed into several different fractions and each particle size is subjected to the interaction of other particles. When non-uniform bed load is transported through channels, not only aggradation and degradation occur, but sorting also occurs in a similar way. Duan and Julien (2005)

concluded that the spatial distribution of particle size in a practical way is highly important for simulation of the river morphological change at a bend section and the particle size parameters are very important. According to Davies and van Rijn (2002) the bed load transport rate is a vital parameter when predicting bed level variation, however all the bed load transport formulae have limited scope of application. In many studies, semi-empirical formulas for simulating bed load transport rates are conducted based on laboratory measurements (El kadi Abderrezzak and Paquier, 2009). However, flow regimes in natural rivers are often unsteady over time, therefore they have generally limited application (Li and Duffy, 2011; Waters and Curran, 2015). Therefore, construction of appropriate empirical formulae for predicting sediment transport rates is an essential consideration for specific cases.

In the present study, semi-empirical formulas for calculating bed load discharge has been constructed by Park *et al*. (2013) is considered the best match to apply because this formula has been constructed based on field data in the natural river bends in South Korea. In this formula, bed load particle size is divided into several fractions. The mean size of each fraction is denoted by d_i where i represents the percent of the fine sediments. The mean particle size of each fraction was input as initial conditions (Duan, 2004; Alho and Makine, 2010; Wu *et al*. 2004a). The bed load discharge is constructed as follows:

$$q_{tbs} = \sum_{i=1}^{N} q_{sbi} \tag{6}$$

$$q_{sb}^{*} = \frac{q_{sb}}{\gamma\sqrt{g(\sigma_s - 1)d^3}} \tag{7}$$

$$q_{sb}^{*} = 0.00157\,\tau_i^{*0.418}\left(\tau_i^{*} - \tau_{ci}^{*}\right)^{0.307} \tag{8}$$

$$\tau_{ci}^{*} = 0.0308\left(\tau_b \frac{d_i}{d_m}\right)^{0.545} \tag{9}$$

$$\tau_i^{*} = \frac{\tau_b}{\gamma(\sigma_s - 1)d_i} \tag{10}$$

where q_{tbs} is the total of bed load discharge; q_{sb}^{*} is the bed load discharge capacity; σ_s is the specific gravity of sediment; d_m and d_i are the grain size of the bed load sediment and i^{th} particle, respectively; τ_{ci}^{*} is the dimensionless Shields stress; τ_b is the bed shear stress (see Fig. 1). τ_b, σ_b, and σ_s are defined by Eq. (11).

$$\begin{aligned} \tau_b &= \gamma h S; \\ \sigma_b &= \left(\frac{d_{84}}{d_{16}}\right)^{1/2} \\ \sigma_s &= \frac{\gamma_s}{\gamma} \end{aligned} \tag{11}$$

where S is the stream slope, γ_s, γ are the specific weight of sediment and water.

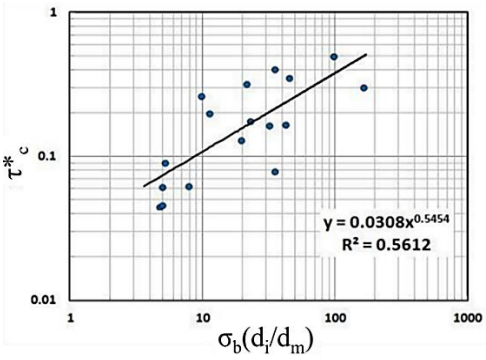

Fig. 1. Relationship between τ^{*}_{c} and σ_b (d_i/d_m) [Park *et al*. 2013].

2.3 Bed Level Variation Equation

Field survey at steep mountain rivers in South Korea showed that when the unit discharge at some rivers is approximately 2.5 m^3/s, the dominant type of sediment movement is bed load. This confirmed that bed loads play important roles in the evolution of steep mountain rivers. Therefore, suspended load is not considered in this work and only bed load is used to simulate degradation or aggradation processes of the river bed. The mass conservation equation of the bed load transport within the mixing layer for each individual size class to calculate the bed level variation is written as follows:

$$\frac{\partial Z_{bi}}{\partial t} + \frac{1}{1-p}\left(\frac{\partial q_{bxi}}{\partial x} + \frac{\partial q_{byi}}{\partial y}\right) = 0 \tag{12}$$

where Z_{bi} is the riverbed elevation; p is the porosity; q_{bxi} and q_{by} are the bed load discharge per unit width

The bed load discharge q_{bxi} and q_{byi} appear in Eq. (12) are determined by Eqs. (13) and (14):

$$q_{bxi} = q_{sbi}\cos\alpha \tag{13}$$

$$q_{byi} = q_{sbi}\sin\alpha \tag{14}$$

where q_{sbi} appears in Eqs. (13) and (14) is determined by Eq. (7). α appears in Eqs. (13) and (14) is determined by Eq. (15).

$$\tan\alpha = \frac{\sin\beta - \frac{1}{f_s\tau^{*}}\frac{\partial z_b}{\partial x}}{\cos\beta - \frac{1}{f_s\tau^{*}}\frac{\partial z_b}{\partial y}} \tag{15}$$

where the shape factor f_s appears in Eq. (15) is calculated by Eq. (16)

$$f_s = 9\left(\frac{d_{50}}{h}\right)^{0.3}\sqrt{\tau^{*}} \tag{16}$$

where quotient d_{50}/h in Eq. (16) is the relative roughness parameter. The term β appears in Eq. (15) is determined by Eq. (17).

$$\beta = \tan^{-1}\left(\frac{v}{u}\right) - \tan^{-1}\left(\frac{A}{r_s}h\right) \tag{17}$$

Where the parameters A and r_s in Eq. (17) are

determined by Eqs. (18) and. (19), respectively.

$$A = \frac{2}{k^2}\left[1 - \frac{n\sqrt{g}}{kh^{1/6}}\right] \tag{18}$$

$$r_s = \frac{|u_i|^3}{\left[u^2\frac{\partial v}{\partial x} + uv\left(\frac{\partial v}{\partial y} - \frac{\partial v}{\partial x}\right) - v^2\frac{\partial u}{\partial y}\right]} \tag{19}$$

The suggested values for A and r_s are 11 and 7, respectively. The slope of horizontal bed often is not large enough to effect on the hydrodynamic processes. Therefore, the role of horizontal bed often is faded in numerous studies (Song *et al.* 2012; Begnudelli *et al*. 2010; Wu *et al.* 2004a).

2.4 Numerical Procedures

The shallow water equations (Eqs. (1), (2) and (3)) are solved numerically by Marker-and-Cell finite difference method (FDM) based on a staggered grid in Cartesian coordinates (Duan, 2004; McKee *et al.* 2008). Where water depth (h) in Eq. (1) is determined at the grid center and q_x, q_y in Eqs. ((2) and (3)) are determined at the cell faces of the grid. The momentum equations (Eqs. (1) and (2)) are discretized to obtain the flow discharge (q_x and q_y) in the x and y directions, respectively at time step (T + 1). Then continuity equation is discretized to obtain new water depth value at time step. The steps in the process of discretizing the sediment transport equation is conducted in a similar way to the momentum equations. The flow and sediment transport module were decoupled for the numerical simulations. To increase forecast accuracy in the morphological changes in a river, morphological evolution is updated after each time step correction by moving the grid cells below a water depth up or down in the case of aggradation or degradation bed.

The numerical solution procedure description given full details can be found by referring to the previous publications (Dang and Park, 2016b).

3. TEST AND VERIFICATION

The first application was obtained from hydraulic laboratory of RCRFIDF (Fig. 1a). The second application was simulated with the bed level variation of the Eosungjun river curved reach after a flood event. To assess the accuracy of the numerical model, several techniques have been developed and widely used to measure certain desirable properties of forecasts with the purpose of assessing their quality (Davies *et al*. 2002). In this work, the model performance assessment was based on the agreement of the simulated results and measured data together with the value of the statistical performance indices such as the Brier Skill Score (BSS) criteria, Root Mean Square Error (RMSE) and Mean Absolute Errors (MAE). BSS and RMSE are the criteria most widely used to assess the model performance with observed data (Dang and Park, 2016b; Davies *et al.* 2002; Guan *et al*. 2016). The BSS has been identified as the most appropriate criteria to determine the performance of the river morphology model (Davies *et al.* 2002) because this criterion compares the model results to a baseline prediction. So, the initial bathymetry is considered as the baseline prediction for river morphology module (Davies *et al.* 2002; Guan *et al*. 2016). The BSS criteria are defined as follows:

$$BSS = 1 - \frac{\sum_{I=1}^{N}\left(Z_b(i,j)_{fie}^{T} - Z_b(i,j)_{sim}^{T}\right)^2}{\sum_{I=1}^{N}\left(Z_b(i,j)_{fie}^{T} - Z_b(i,j)_{sim}^{T=0}\right)^2} \tag{20}$$

where Z_b is the local bed elevation, subscript "fie" and "sim" refer to field data and simulated results, N is the total number of cells and T is time step

General quality characterizations of the BSS criteria are shown in Table 1.

Table 1. Classification ranges for BSS values [Davies *et al*. 2002]

Classification ranges	Brier Skill Score
Excellent	1.0–0.8
Good	0.8–0.6
Reasonable	0.6–0.3
Poor	0.3–0.00

RMSE also known as a Root Mean Square Deviation (RMSD) is one of the most widely used statistics (Davies *et al*. 2002; Guan *et al*. 2016). It is often used for comparing the results of numerical simulation and measurement data.

The expression for calculating the RMSE is defined as follows.

$$RMSE = \sqrt{\frac{1}{n}\sum_{i=1}^{N}\left(x_{obs} - x_{cal}\right)^2} \tag{21}$$

where X_{obs}, X_{cal} are the measured and predicted values, respectively

3.1 Degradation of a Curved Channel Bed

First, the experimental channel was applied to evaluate the performance of the developed model by simulating the flow hydrodynamic and bed level changes. The experiment flume was conducted to carry out the unsteady flow where the experiment flume shape was designed similar as a natural channel. An experimental channel was carried out in 14.0m long, 1.5m wide, with a horizontal bed and vertical sidewalls and the rotation angle was 90-degree central bends with a radius of curvature of 2.5m that connects the inflow and outflow straight channel section reaching 4.5m (Fig. 2).

To investigate the process of the bed degradation, final bed profile of the experimental flume was investigated without sediment being fed at the inflow channel end. In this study case, the numerical model was used to predict for simple bed topography. Therefore, only three-grain size fractions of bed load (including d_{35}, d_{50}, and d_{85})

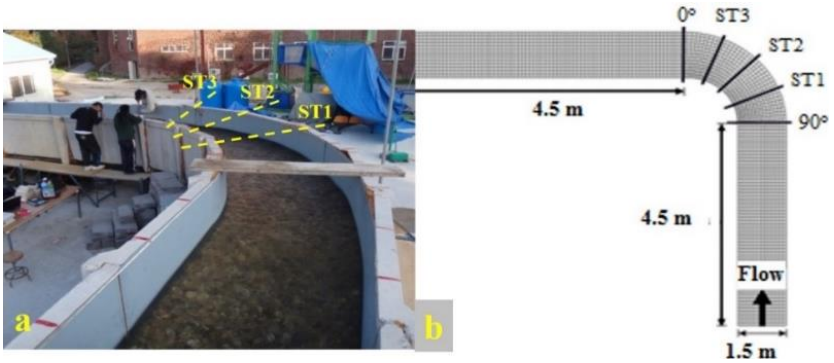

Fig. 2. Schematic plan and specifications of the experimental channel.

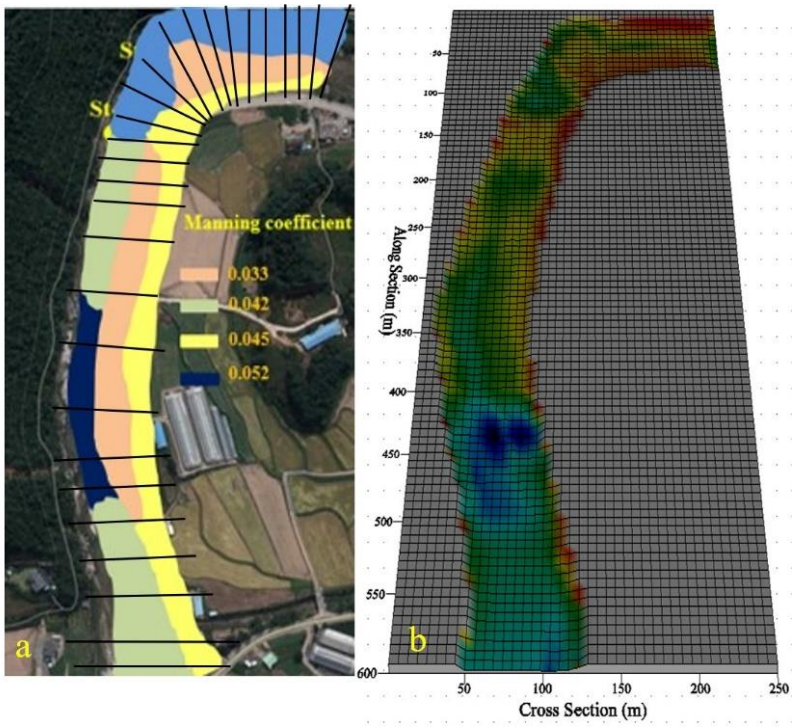

Fig. 3. Schematic plan and roughness zones of the study river reach.

were applied. For flow depth adjustment at the curve entrance, a sluice gate was established at

3.2 Bed Level Variation in the Eosungjun Curved River Reach

In this case, the study area was a short section of Yangyang Namdea river which is located in Gangneung Province (South Korea) (Fig. 3). The curved river reach was carried out in 600 m long and width varies from 50 m to 75 m with bed slope in the range of 1.25% to 2.2%. Field surveys to collect the bed topography data at the curved river reach before and after the flood event at 40 cross sections were performed using the levelling measuring device. Bed topography data were designed in the form of points, where x, y, and z are corresponding to the longitude, latitude, and depth respectively. Field surveys also pointed out that the riverbed aggradation and degradation process occurred at the curved river reaches during flood event and the bed material is predominantly included of sand, gravel and cobble, etc. The mean size curve of the bed material analyses was shown in Fig. 4. The hydrograph data of water level with a 10 minutes interval was collected at the Jinam Bridge station from January 2012 to December 2012 as input boundary data (Fig. 5). In addition, the measured time series of sediment discharge at the inflow boundary was also established as boundary conditions. The study river reaches has complex geometrical features, the Manning's coefficient

the outflow end to control flow depth that maintain the water depth in the similar state as the original water surface. The experimental data were established and measured over a period of 60 min with the following specific conditions. Hydrographs of the flow discharge were established as the inflow boundary with base flows of 190 l/s, which was equivalent to the incipient motion condition of the median grain size and maximum

peak flows of 212 l/s with a time interval of Dt = 1.0s, the averaged flow velocity 0.85 m/s were provided as the inflow boundary condition, and the averaged depth 0.15m was provided. The computational mesh was 140×15nodes. Median diameter: d_{35} = 2.1cm, d_{50} = 3.4cm and d_{85} = 4.5cm; bed slope was in the range from 1.05 to 1.5% and porosity: p = 0.35; the time step for the sediment simulations was 10s. The current model allows the specifications for the Manning's coefficient for each grid cell. In this case, the experimental flume has simple geometrical features, the Manning's coefficient therefore was established as a constant (n = 0.015).

therefore, was calculated for each cell (Fig. 3a). Grid spacing with 1.0m×1.0m resolution was constructed based on the measured raw data using Digital Terrain Models (DTMs). Field surveys recorded that most of the time, the water level was lower than 0.5 m (Fig. 5). Field evidence demonstrated that the bed aggradation and degradation process induced by low water level was insignificant. In addition, the model sensitivity to the water level was performed and the analysis results indicated that when the recorded water level at inflow boundary was lower than 0.5 m, the study area do not have a significant contribution to bed aggradation and degradation process. Therefore, to save computational time the study only focuses on the water level which was equal to or higher than a threshold of 0.5 m.

This threshold value corresponds to the flood period from 17-21 Sep 2012. Thus, the simulation period was selected from 17-21 Sep 2012 with time step for flow and sediment simulations of 1.0s and 30s, respectively.

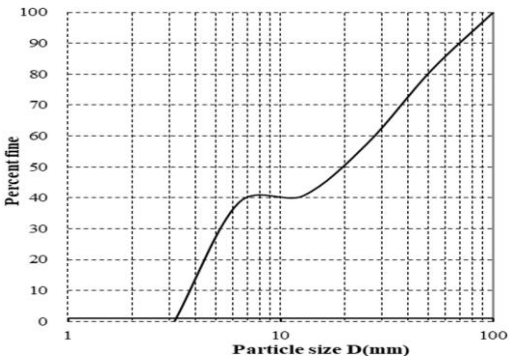

Fig. 4. Grain size distribution curves of the bed material.

Therefore, instead of just using a value of the median grain diameter, the bed material sizes in this study were divided into several fractions, corresponding to the diameter D_i and this method also has been used by Wu *et al.* (2004a); Guan *et al.* (2016); Wilcock and Crowe (2003). The bed load transport rate is calculated for each grain size based on the collected data from Fig. 6. The total bed load discharge was then calculated by Eq. (6) as the summation of the fractional transport rates. In most studies, the numerical models only set up the bed load size by applied median grain diameter (d_{50}) (El kadi Abderrezzak and Paquier, 2009; Hung *et al.* 2009; Li and Christopher, 2011). In this work, particle size analysis performed using United States Standard Size test sieves showed that the riverbed was composed sand, gravel, cobbles and boulders.

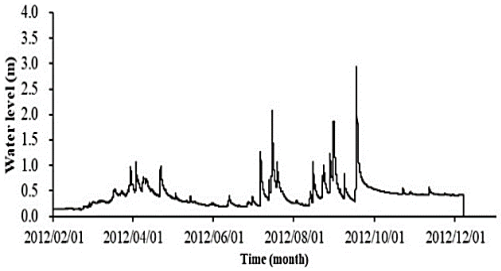

Fig. 5. The water level at the inflow boundary.

4. RESULTS AND DISCUSSION

4.1 Curved Channel Case

The simulation results of the flow velocity distribution (Fig. 3) pointed out the flow velocity increased along the outer bank and decreased along the inner bank. These results were consistent with other study, which have been previously published by Duan (2004); Guan *et al.* (2016).

The simulation results were a small difference with the measured data at ST1, ST2, ST3 cross sections during the simulation period. Comparison of calculation results and measurement data through the RMSE values at ST1, ST2, ST3 cross sections were 0.05, 0.045 and 0.042, respectively. This means that the simulated model of the flow was in good agreement with the field data.

The comparison between the simulated results and measured bed level at ST1, ST2 and ST3 cross sections were shown in Fig. 2b. Field survey showed that the experimental flume was a slight degradation during simulation run time (Fig. 7).

Figure 7 indicates a comparison of simulated results and measured bed level at ST1, ST2 and ST3 cross sections of the experimental flume. The average degradations at ST1, ST2 and ST3 cross sections were determined to be approximately 0.048 m, 0.085 m and 0.123 m respectively compared with the original bed and the simulated results were 0.061 m, 0.071 m and 0.107 m, respectively. Similarly, the minimum degradation occurred at ST1 cross section measured was 0.048 m compared to the original bed while the corresponding value of the numerical model was 0.056 m.

In contrary, the maximum degradation occurred at ST3 cross-section measured was 0.123 m while model calculated was 0.107 m (Table 2). The validation of the field data and predicted bed level at ST1, ST2, ST3 cross sections using the BSS criteria corresponds to the values of 0.93, 0.89, and 0.91, respectively.

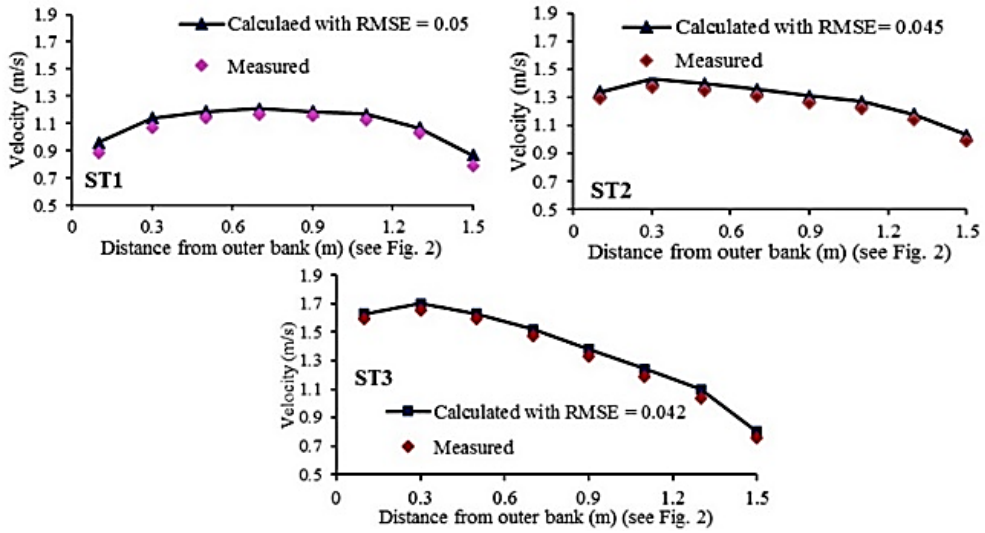

Fig. 6. Comparisons of simulated velocity and field data at ST1, ST2 and ST3 cross sections.

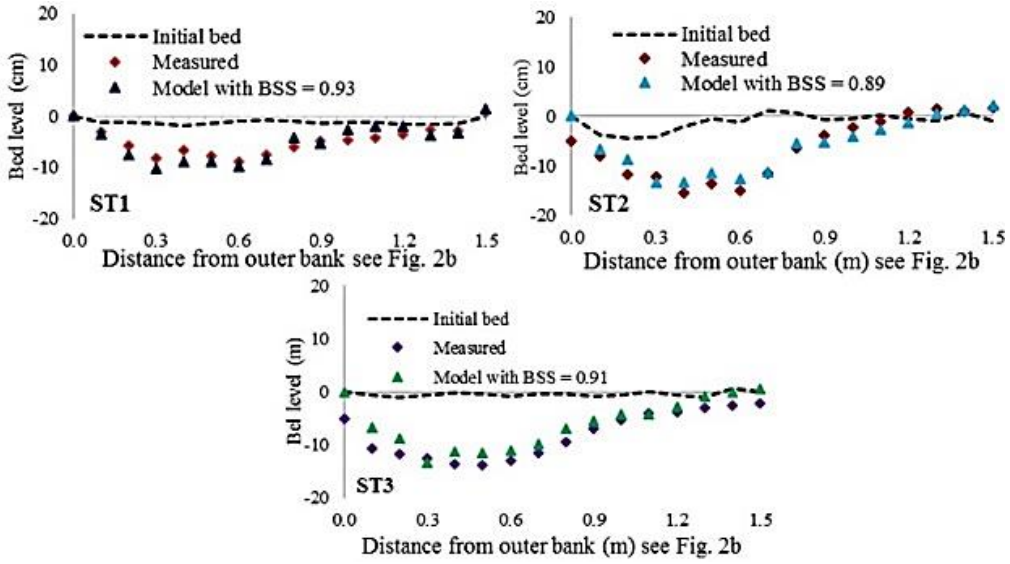

Fig. 7. Variations in cross section bed profiles with time at t = 60 minute.

Table 2 Comparison of field data and simulated bed level at the ST1, ST2 and ST3

Cross sections	Measured (m)	Calculated (m)
ST1	-0.048	-0.056
ST2	-0.085	-0.071
ST3	-0.123	-0.107

Note: (-) is bed degradation, (+) is bed aggradation

4.2 Eosungjun Curved River Case

To create convenience for analysis of the results, the study river reach was subdivided into the three sub-reach: the first straight river reaches (entrance to No.18 cross section), the next curved river reaches (from No.20 to No.28 cross section) and the final straight river reaches (from No.29 to No.36 cross section) are pointed out in Fig. 3a. The simulated results pointed out that bed level at the first straight river reach after the flood event was a slight degradation. The simulated degradation depth was in a range of 0.124-0.156 m which has a same magnitude to the field data.

A comparison at No.12, No.14, No.16 and No.18 cross sections also showed that the developed model shows a similar profile shape with the measured data, i.e. degradation occurs at the outer bank of the bend. Field survey after the flood event showed that the average degradations at No.12, No.16 and No.18 cross sections were determined to be approximately 0.113m, 0.102m, and 0.121m, respectively compared to the original bed while the developed model calculated were 0.156m, 0.124m, and 0.148m, respectively. In contrary, field data also showed that a slight aggradation occurred at No.14 cross section after the flood event (Table 3).

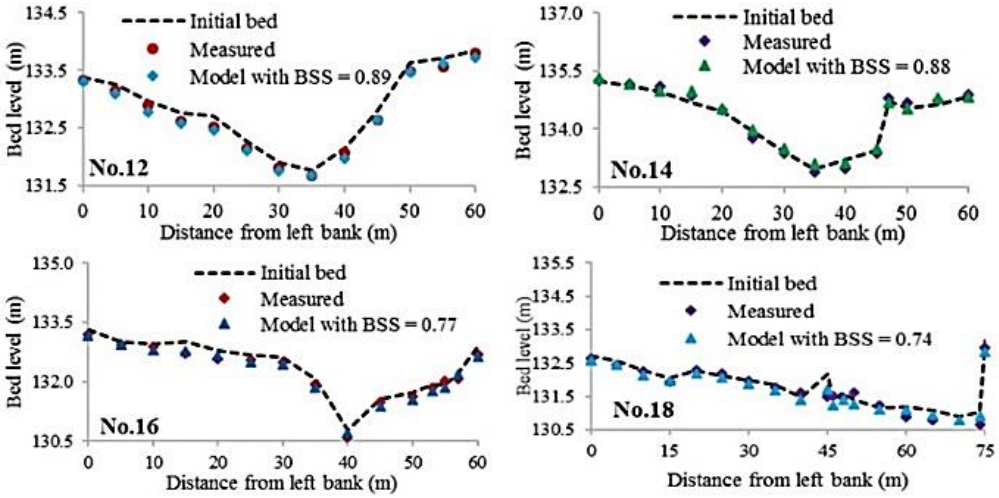

Fig. 8. Comparison of field data and simulated bed level at No.12, 14, 16 and No.18 cross sections.

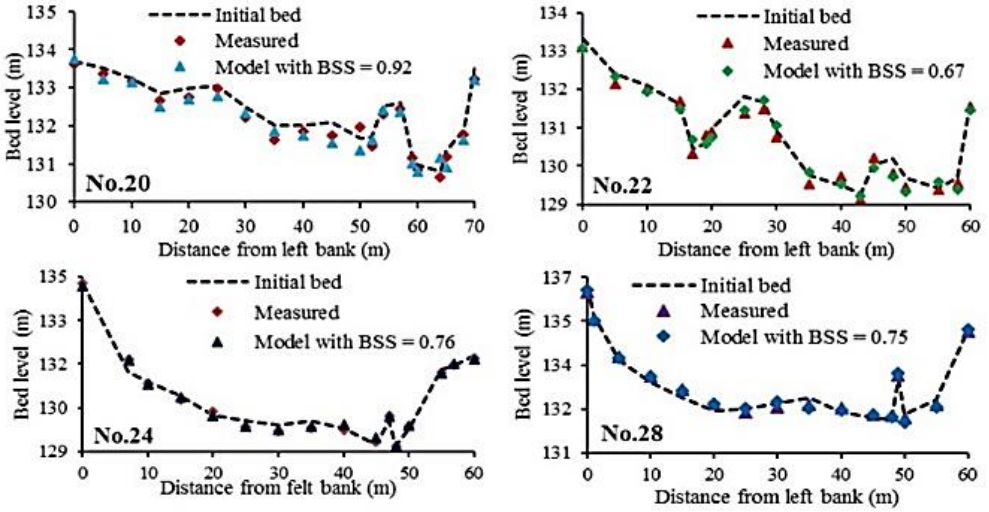

Fig. 9. Comparison of field data and simulated bed level at No.20, No.22, No.24 and No.28 cross sections.

Table 3 Comparison of field data and simulated bed level at No.12, 14, 16 and No.18 cross sections

Cross sections	Measured (m)	Calculated (m)
No.12	-0.113	-0.156
No.14	-0.085	+0.023
No.16	-0.102	-0.124
No.18	-0.121	-0.148

The average aggradation was carried out to be approximately 0.016 m compared to the original bed while the model calculated was 0.023 m. The BSS values corresponding to the results of the predicted model and field data at No.12, No.14, No.16 and No.28 cross sections were 0.89, 0.88, 0.77 and 0.74 (Fig. 8), which means there was a fairly good agreement between simulated results and field data compared to qualification ranges for the BSS.

Similarly, the simulated results showed that the curved river reach (from No.20 to No.24 cross section) had a strong degradation, except at No.28 cross section which only had a slight aggradation. Field survey after the flood event showed that the average degradations at No.20, No.22 and No.24 cross sections were determined to be approximately 0.161m, 0.117m and 0.14m respectively compared to the original bed while the developed model were 0.192m, 0.109m and 0.15m respectively. In contrary, the average aggradation at No.28 cross section measured was approximately 0.16m compared with the original bed value which was 0.17m using the developed model (Table 4).

Table 4 Comparison of field data and simulated bed level at No.20, 22, 24 and No.28 cross section

Cross sections	Measured (m)	Calculated (m)
No.20	-0.161	-0.192
No.22	-0.117	-0.109
No.24	-0.142	-0.157
No.28	+0.163	+0.171

The values of the BSS criteria corresponding to the results of the measured data and developed model at No.20, No.22, No.24 and No.28 cross sections were 0.92, 0.67, 0.76 and 0.75 (Fig. 9).

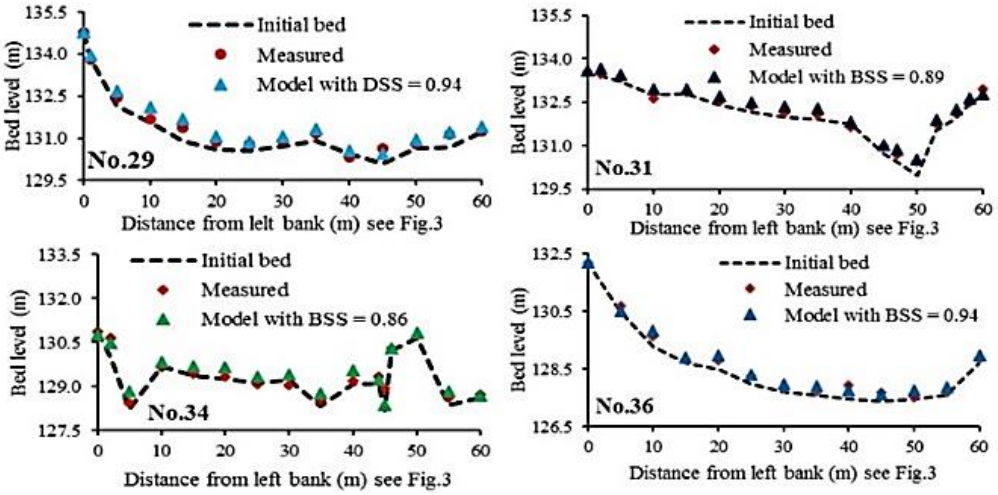

Fig. 10. Comparison of field data and simulated bed level at No.29, No.31, No.34 and No.36 cross sectionsSpecifically, at the straight river reach (from entrance to No.18 cross section), only several locations were eroded and the average degradation depth was calculated 0.101m.

Finally, the simulated results showed that the river reach from No.29 to No.36 cross section had an aggradation. Survey data after the flood event showed the average aggradations at No.29, No.31, No.34 and No.36 cross sections were measured to be approximately 0.207m, 0.152m, 0.16m and 0.198m respectively compared with the original bed while the simulated results were 0.256m, 0.276m, 0.332m and 0.271m respectively (Table 5) with the BSS values were 0.94, 0.89, 0.86, and 0.94, respectively (Fig. 10).

Table 5 Comparison of field data and simulated bed level at No.29, 31, 34 and No.36 cross sections

Cross sections	Measured (m)	Calculated (m)
No.29	+0.207	+0.256
No.31	+0.153	+0.276
No.34	+0.161	+0.332
No.36	+0.198	+0.271

Generally, the results of the simulated model and field survey pointed out that aggradation and degradation processes were mixed together throughout the entire river reach.

The maximum degradation depth occurred at No.12 cross section near the right bank was calculated 0.156 m; at the curved river reach (from No.20 to No.28 cross section), the riverbed was changed with the following typical morphological changes: degradation strongly dominated and appeared near the right bank where the rate of bed degradation was higher than left bank, the average degradation depth was estimated to be approximately 0.072m while the maximum degradation depth was 0.39m near the right bank; at the final straight river reach (from No.29 to No.36 cross section) while aggradation occurred and dominated on both sides of the river bank with average aggradation depth was calculated 0.266m and the maximum aggradation depth was 0.440m at No.34 cross section and occurred near the left bank. Comparison of the simulated results and field data based on the values of the BSS on the entire study reach was in the range of 0.67 to 0.94. This confirmed that the developed model predicts the river morphological changes reasonably well. The study results were fully consistent with other studies, which have been previously published by Guan *et al*. (2016).

4. CONCLUSION

The research constructed a 2D model with grain size fractions and was tested to an experiment channel case and the natural river bends. New formulation was proposed for predicting bed load sediment discharge with grain size fractions. The developed model has well predicted the river morphological changes for both experimental flume and natural river bend with a common feature, whereby river bed at the outer bank was eroded and inner bank was deposited. Simulation results for both experimental flume and natural river bend showed that degradation mainly occurred at the outer bank and aggradation occurred at the inner bank of the river bend. Simulation results confirm that depth-averaged 2D model with the use of particle size fractions in the sediment transport module could be applied to predict the river morphological change in the natural bend that grain size fractions are considered.

Two-dimensional model could be sufficiently reliable for simulating hydrodynamics and morphological change in the natural bend and this can save simulation time of the model.

The advantages of the constructed model:The subdivision of bed load sediment into several size fractions and establish different values of Manning coefficients for each zone in computational domain The constructed model admits the user to intervene favorably the simulation procedure The limitations of the developed model are:The computational grid

is established by complicated process It is difficult to determine the sensitivity of the parameters to the morphological changes; It is not easy to calibrate the parameters of the constructed model when simulating the morphological changes.

ACKNOWLEDGMENTS

We are very grateful to Prof. Park Sang Deog, Gangneung-Wonju National University, South Korea for supporting the database.

REFERENCES

Alho, P. and J. Mäkine (2010). Hydraulic parameter estimations of a 2D model validated with sedimentological findings in the point bar environment, *Hyd.Processes* 24(18), 2578-2593.

Barbhuiya, A. K. and S. Talukdar (2010). Scour and 3D turbulent flow fields measured by ADV at a 90-degree horizontal forced bend in a rectangular channel, *Flow Measurement and Instrumentation* 21(3), 312-321.

Begnudelli, L., A. Valiani and B. F. Sanders (2010). A balanced treatment of secondary currents, turbulence and dispersion in a depth-integrated hydrodynamic and bed deformation model for channel bends, *Advances in Water Resources* 33(1), 17-33

Bhallamudi, S. M. and M. H. Chaudhry (1991). Numerical Modeling of Aggradation and Degradation in Alluvial Channels, *J Hydraulic Eng*, 117(9).

Bravo-Espinosa, M., W. Osterkamp and V. Lopes (2003). Bedload transport in alluvial channels, *J Hydraul Eng*, 10(783), 783–795.

Dang, T. A. and S. D. Park (2016b). Experimental analysis and numerical simulation of bed elevation change in mountain rivers, *SpringerPlus*.

Darby, S. E., A. M. Alabyan and M. J. Van De Wiel (2002). "Numerical simulation of bank erosion and channel migration in meandering rivers", *Water Resources Research* 38(9), 1163.

Davies, A. G., L. C. van Rijn, J. S. Damgaard, J. Graaff and J. S. Ribberink (2002). Intercomparison of research and practical sand transport models, *Coastal Eng*. 46, 1-23.

Duan, J.G. (2004). Simulation of flow and mass dispersion in meandering channels, *J. of Hydraul*. Eng., 130(10), 964-976.

Duan, J. G. and P. Y. Julien (2005). Numerical simulation of the inception of meandering channel, *Journal of Earth Surface Processes and Land Forms* 30, 1093-1110.

Elkadi Abderrezzak, K. and A. Paquier (2009). One-dimensional numerical modeling of sediment transport and bed deformation in open channels, Water Resour. Res., 45, W05404.

Guan, M., N. G. Wright, P. A. Sleigh, S. Ahilan and R. Lamb (2016). Physical complexity to model morphological changes at a natural channel bend, *Water resources research*.

Hung, M., T. Hsieh, C. Wu and J. Yang (2009). 2D non-equilibrium non-cohesive and cohesive sediment transport model, *J Hydraul Eng*, 135(5), 369–382

Kasvi, E., P. Alho, E. Lotsari, Y. Wang, A. Kukko, H. Hyyppä and J. Hyyppä (2015). 2D and 3D computational models in hydrodynamic and morpho-dynamic reconstructions of a river bend: sensitivity and functionality, *Hydrological Processes* 29(6), 1604-1629.

Khosronejad, A. C., S. Rennie, N. Salehi and R. Townsend (2007). 3D numerical modeling of flow and sediment transport in laboratory channel bends, *Journal of Hydraulic Engineerin*g 133(10), 1123-1134.

Lane, S. N., K. F. Bradbrook, K. S. Richards, P. A. Biron and A. G. Roy (1999). The application of computational fluid dynamics to natural river channels: 3D versus two-dimensional approaches, *Geomorphology* 29(1–2), 1-20.

Li, S. and C. J. Duffy (2011). Fully coupled approach to modeling shallow water flow, sediment transport, and bed evolution in rivers, *Water Resources Research* 47, W03508.

McKee, S., M. F. Tome, V. G. Ferreira, J. A. Cuminato, A. Castelo, F. S. Sousa and N. Mangiavacchi (2008). The marker and cell method, *J. Comput Fluids* 37:907-930.

Miglio, A., R. Gaudio and F. Calomino (2009). Mobilebed aggradation and degradation in a narrow flume: laboratory experiments and numerical simulations, *Hydro-environ Res* 3,9-19.

Park, S. D., S. W. Lee and K. D. Han (2013). Development of technique estimating sediment load in mountain river, *MOLIT final report, land transport report R&D/B-01* 275-278.

Paulo, G. S., M. F. Tom and S. McKee (2007). A marker-and-cell approach to viscoelastic free surface flows using the PTT model, *J. Non-Newton Fluid Mech* 147, 149–174.

Song, C. G., I. W. Seo and Y. D. Kim (2012). Analysis of secondary current effect in the modeling of shallow flow in open channels, *Advances in Water Resources* 41(0), 29-48.

Wang, D., P. Tassi, K. E. Abderrezzak, A. Mendoza, J. D. Abad and A. Langendoen (2014). 2D and 3D numerical simulations of morphodynamics structures in large-amplitude meanders, *River Flow*.

Waters, K. A. and J. C. Curran (2015). Linking bed morphology changes of two sediment mixtures to sediment transport predictions in unsteady flows, *Water Resources Research* 51(4), 2724-2741.

Wilcock, P. and J. Crowe (2003). Surface-based transport model for mixed-size sediment", *Journal of Hydraulic Engineering* 129(2), 120-128.

Wu, B. S., A. Molinas and P. Y. Julien (2004a). Bed-material load computations for nonuniform sediments, *J. Hydraul. Eng.*, 130, 1002-1012.